Natural Resources for Human Health

eISSN: 2583-1194

Original Research

Received 24 July 2026
Revised 30 Aug 2026
Accepted 18 Sep 2026

Natural Resources for Human Health 2026, Vol. 6 (21s): 645–665

KEYWORDS:
polycystic ovary syndrome; Nyctanthes arbor-tristis; Polyalthia longifolia; network pharmacology; AutoDock Vina; PPARG; steroid hormone biosynthesis.

Integrative Network Pharmacology and Molecular Docking Analysis of Nyctanthes arbor-tristis and Polyalthia longifolia for Potential PCOS Therapy

Yashika Saini[1], Dr. Meena Godha[1], Dr. Dipender Singh[2]

[1]School of Life and Basic Sciences, Jaipur National University, Jaipur, Rajasthan, India, 302017.
[2]Department of Forensic Medicine and Toxicology, Govt Medical College, Sawai Madhopur, Rajasthan, India, 322001.
ORCID iD: Yashika Saini https://orcid.org/0009-0006-6780-0952; Dr. Meena Godha https://orcid.org/0000-0002-6247-8021; Dr. Dipender Singh https://orcid.org/0009-0008-2964-0091

ABSTRACT: Polycystic ovary syndrome (PCOS) is characterized by interrelated reproductive, endocrine and metabolic disturbances. This study integrated phytochemical screening, protein-target prediction, protein–protein interaction (PPI) analysis, Gene Ontology (GO) and Kyoto Encyclopedia of Genes and Genomes (KEGG) enrichment, and molecular docking to investigate bioactive constituents of Nyctanthes arbor-tristis and Polyalthia longifolia. Four P. longifolia compounds and nyctanthic acid from N. arbor-tristis were prioritized. The compound–disease analysis identified 68 and 37 overlapping PCOS-associated targets, respectively, with PPARG and TNF prominent in both PPI networks. Steroid hormone biosynthesis was enriched in P. longifolia (12 genes; Benjamini-adjusted $p = 1.18 \times 10^{-10}$) and N. arbor-tristis (nine genes; adjusted $p = 1.27 \times 10^{-8}$). The PPAR signaling pathway included six genes in each plant-specific target set (adjusted $p = 0.00378$ and 0.000905, respectively). Fifteen ligand–protein docking complexes were examined using AutoDock Vina. Among the four CID-labelled ligands, minimum docking scores of −8.4 kcal/mol occurred in the 1TNF and 1XP1 complexes; a fifth ligand yielded a score of −7.6 kcal/mol with 9V8G. Residue-level interaction profiles included an ASP351 hydrogen bond in 1XP1 and GLN470 contacts in 9V8G. The combined results identified candidate steroidogenic and metabolic mechanisms that merit targeted biochemical and cellular evaluation.

1. INTRODUCTION

Polycystic ovary syndrome (PCOS) is an endocrine condition that has a complex and heterogeneous nature in women of reproductive age, associated with reproductive, hormonal and metabolic abnormalities. The main clinical symptoms are hyperandrogenism, ovulatory insufficiency, irregular menses and polycystic ovarian morphology. Besides reproductive disorders, insulin resistance, obesity, dyslipidaemia and high cardiovascular risk are common findings with PCOS. The international guidelines based on evidence strongly state that PCOS should be assessed and treated on a case-by-case basis due to the variation in clinical symptoms and complications in PCOS patients (Teede et al., 2023). The etiology of PCOS is multifactorial rather than single molecular abnormality, as it involves interplay of genetic, endocrine, metabolic and environmental factors (Escobar-Morreale, 2018). In addition, it has been reported that genome-wide association studies have revealed several susceptibility genes linked to PCOS, which suggests that several coordinately acting genes are also involved in the development of PCOS (Day et al., 2018).

Due to the multifactorial nature of PCOS, there are difficulties in developing therapeutic strategies that can address the multiple pathological alterations of PCOS. Traditional practices focus on the control of hormonal disorders, enhancement of metabolic function, restoration of ovulation and minimization of future complications. But because of the interdependency between reproductive and metabolic dysfunction, it is important to explore other molecular mechanisms and candidate therapeutic compounds. Network pharmacology is a novel system's biology paradigm, which studies more than one compound, molecular target, and signaling pathway at once, thereby analyzing interactions between various components of the biological system (Hopkins, 2008). This strategy is especially applicable to PCOS as changes in the production of steroid hormones, insulin, lipid metabolism, and inflammatory responses can act synergistically to promote disease progression. Combining network pharmacology with molecular docking can thus help uncover complementary information on the possible compound–target interaction and structural properties (Cheng et al., 2025; Abomughaid, 2026).

Medicinal plants are one of the major sources of structurally diverse phytochemicals which could be explored for their biological activities. Recent advancements in phytochemical databases and computational screening techniques have enabled the identification of plant constituents in a systematic manner and their potential molecular targets. Indian Medicinal Plants Phytochemistry and Therapeutics (IMPPAT) is a curated database of phytoconstituents of Indian medicinal plants and for facilitating computational phytochemical investigations (IMPPAT 2.0, 2023). In the present study, *Nyctanthes arbor-tristis* and *Polyalthia longifolia* were chosen for further study on the molecular relevance of their phytoconstituents to the biological pathways associated with PCOS. A computational approach was used to perform an integrated physicochemical screening, target prediction, protein interaction analysis, functional enrichment, and molecular docking of the selected compounds.

Computational evaluation of pharmacokinetic properties is a key pre-step in identifying phytochemicals that should be further studied at the molecular level. SwissADME predicts physicochemical properties, pharmacokinetic parameters, drug-likeness and medicinal chemistry characteristics, which allows for a systematic evaluation of the small molecules in early-stage screening (Daina et al., 2017). After the identification of a compound, SwissTargetPrediction allows to predict potential protein targets, based on the molecular similarity and known ligand-target relationship (Daina et al., 2019). Molecular weight, lipophilicity, solubility and permeability are physiochemical properties that will affect drug absorption and distribution in vivo and are important factors to consider in compound prioritization (Lipinski et al., 1997). Computational toxicity assessment is used to obtain more data on potential toxic liability. ProTox 3.0 can be used to predict toxicity-related endpoints, and can be used to perform preliminary safety-related screening of chemical compounds (Banerjee et al., 2024). These computational tools constitute an organized procedure to identify phytoconstituents and assess their potential for further biological studies.

Identification of molecular targets for PCOS serve as a critical link between the predicted phytochemical activities and disease related biological processes. Protein–protein interaction analysis (PPI) helps to study relationships between different proteins and aids in determining targets with high levels of connectivity in molecular networks. STRING links experimental observations, curated databases and computational predictions to capture associations between proteins and their functional relationships (Szklarczyk et al., 2023). These interaction networks can be plotted and analyzed with Cytoscape, which has tools to analyze molecular connectivity and find proteins that are central to biological networks (Shannon et al., 2003). These analyses can be helpful for ranking molecular targets linked to endocrine control, metabolic homeostasis and inflammatory signaling, but not for the direct determination of compound-protein binding.

Further information regarding the biological relevance of identified molecular targets is provided by functional enrichment analysis. Selected genes set can be analysed for enriched biological functions and molecular pathways using the Database for Annotation, Visualization and Integrated Discovery (DAVID) (Sherman et al., 2022). The biological associations that are obtained through Gene Ontology (GO) enrichment are classified in three categories: biological processes, cellular components, and molecular functions (The Gene Ontology Consortium, 2019); Kyoto Encyclopedia of Genes and Genomes (KEGG) analysis identifies pathways represented by the selected targets. Enrichment analysis is a multi-test approach, so multiple comparison adjustment is required to reduce the false discovery rate and to facilitate a valid statistical interpretation (Benjamini and Hochberg, 1995). By using both functional enrichment and protein interaction analysis, they can identify potential important biological pathways that can provide clues to the mechanisms involved in the association between the phytochemical targets and PCOS.

In addition to network-based investigations, molecular docking is also performed to study the possible interactions between a phytochemical and selected protein structure. AutoDock Vina is a computational tool for assessing the conformations of a

ligand and finding favourable orientations for the binding site within a protein-binding region (Trott and Olson, 2010). The advances in AutoDock Vina have led to an improvement in the docking capabilities and in the ways by which ligand–receptor interactions may be explored (Eberhardt et al., 2021). Docking analysis allows for the analysis of predicted binding affinities and molecular contacts including hydrogen-bond, hydrophobic and electrostatic contributions. The structural observations can be useful in prioritising selected compounds and targets for further investigation.

The interpretation of the biological relevance of the candidate molecular targets of PCOS requires a thorough knowledge of the endocrine and metabolic mechanisms involved. PCOS is characterized by abnormalities in ovarian steroidogenesis, regulation of androgen, insulin response, and reproductive endocrine signaling (Azziz et al., 2016). Changes in these pathways have been linked with the diverse clinical features of the disorder, and the interaction between these pathways is thought to be part of the complex pathophysiology of the disorder (Dumesic et al., 2015). Disease-related gene resources like GeneCards can be used to identify and structure genes that may be associated with these disease processes (Stelzer et al., 2016). The standardized biological annotations provided by the Gene Ontology help to interpret the functions of gene products, while the protein sequence and function information provided by UniProt can help in the characterization of selected molecular targets. Combining these resources allows systematic examination of the connections between the disease-associated genes, the biological pathways and the phytochemical targets.

Structural information is especially critical if prospective molecular targets are identified for docking studies. The RCSB Protein Data Bank (RCSDb) contains experimentally-determined three-dimensional (3D) structures of biological macromolecules, which are used for structure-based studies of ligand recognition and protein interactions (Burley et al., 2021). Chemical structure conversion and molecular file preparation for computational investigations are made easier with the use of molecular preparation tools like Open Babel (O'Boyle et al., 2011). However, limitations of the scoring functions, flexibility of the receptor, conformational differences of the ligands, and the difference between predicted binding affinity and experimentally observed biological activity should be considered when interpreting the molecular docking results (Warren et al., 2006; Che and Zhang, 2025). It is therefore important to combine structural observations with the results from network pharmacology to establish a more comprehensive basis for prioritizing biologically relevant compound–target interactions.

Five phytoconstituents, four from *Polyalthia longifolia*, namely (4E,7E)-1,5,9,9-tetramethyl-12-oxabicyclo [9.1.0] dodeca-4,7-diene, 6-epi-β-bisabolol, 4,8-β-epoxycaryophyllene and kolavenic acid, and one from *Nyctanthes arbor-tristis*, namely nyctanthic acid, were selected for the integrated analysis in the present investigation. Sixty-eight common targets associated with PCOS were found in *P. longifolia* and 37 common targets were found in *N. arbor-tristis*. Protein interaction analysis identified several interesting targets, such as PPARG, TNF, ESR1, PPARA, MAPK3, and proteins related to the regulation of steroids. Functional enrichment revealed biological associations related to steroid hormone biosynthesis, androgen metabolism, steroid binding and PPAR signaling. These results led to structural studies of these targets in search of molecular targets for drug development.

Selected receptor structures were then used with molecular docking to analyze the possible interactions between the ligands and the receptor. The crystal structure of the human estrogen receptor alpha (PDB ID 1XP1) ligand binding domain serves as a structural template for studying interactions of importance to the estrogen receptor biology (RCSB Protein Data Bank, 2004). Likewise, another nuclear receptor, involved in metabolic regulation, the PPAR gamma ligand-binding domain (PDB ID 9V8G) can be structurally evaluated for candidate ligands (RCSB Protein Data Bank, 2025). These docking studies, along with the other selected protein structures, were employed to assess the predicted binding affinities and interaction profile for the prioritized phytoconstituents. The combination of docking results with network pharmacology and enrichment analysis could serve as a method to study the potentially relevant molecular relationships in PCOS.

Based on this, the present study was conducted to explore the possible molecular mechanism of phytoconstituents of *Nyctanthes arbor-tristis* and *Polyalthia longifolia* against PCOS by using a network pharmacology and molecular docking integrated approach. We analyzed the phytochemical constituents, ADME and toxicity properties, predicted compound-associated protein targets, overlapping PCOS associated genes, PPI network analysis, GO and KEGG enrichment analysis, and molecular docking interactions. The aim of this study was to establish these complementary computational approaches to identify compounds, molecular targets, and biological pathways that could help in understanding the possible therapeutic relevance of the selected phytoconstituents and give a scientific basis for the next experimental validation.

Natural Resources for Human Health
eISSN: 2583-1194

2. MATERIALS AND METHODS

2.1 Integrated computational workflow

The research workflow consisted of phytochemical identification, drug-likeness and bioavailability screening, toxicity prediction, target identification, intersection with PCOS-associated genes, PPI network construction, GO/KEGG enrichment, and molecular docking with interaction mapping. **Figure 1** presents the sequence of analyses.

Compound selection	Target prioritization	Pathway and docking interpretation
IMPPAT → SwissADME → ProTox	SwissTargetPrediction → GeneCards → STRING	DAVID GO/KEGG → AutoDock Vina → 2D/3D interaction maps

Figure 1. Integrated computational workflow for phytochemical screening, target identification, functional enrichment and molecular docking.

2.2 Phytochemical identification and screening

Plant-associated phytochemicals were identified using IMPPAT and screened for molecular weight, drug-likeness (DL) and bioavailability (BA) scores using the compiled screening data. The specified thresholds were DL > 0.18 and BA > 0.30. Nyctanthic acid (DL = 0.18) was included at the selection boundary. The final panel comprised four *P. longifolia* constituents and one *N. arbor-tristis* constituent. Predicted toxicity endpoints were assessed as preliminary risk indicators rather than experimental safety measurements (Daina et al., 2017; Lipinski et al., 1997).

2.3 Predicted target identification, PPI and pathway enrichment

Predicted protein targets were standardized by gene symbol (The UniProt Consortium, 2023) and compared with PCOS-associated genes retrieved from GeneCards. The analyses identified 68 intersecting targets for *P. longifolia* and 37 for *N. arbor-tristis*. Protein associations were investigated through STRING, and network connectivity was used to prioritize candidate hubs (Szklarczyk et al., 2023). Gene Ontology biological process, cellular component and molecular function annotations, together with KEGG pathway enrichment, were evaluated through DAVID. Benjamini-adjusted p-values were used to assess statistical enrichment at a threshold of $p < .05$ (Sherman et al., 2022; Benjamini and Hochberg, 1995). Target-class output plots for each of the five shortlisted phytoconstituents were also reviewed descriptively to summarize the distribution of predicted target classes; these class profiles were treated as broad computational predictions and not as PCOS-specific target intersections.

2.4 Molecular docking and interaction analysis

AutoDock Vina was used to examine ligand placement in selected protein-binding regions and calculate docking scores (Trott and Olson, 2010; Eberhardt et al., 2021). Four ligands (PubChem CIDs 6441458, 12300148, 22559443 and 91749887) were docked against 1TNF, 1XP1 and 9V8G, producing 12 complexes. An additional ligand was evaluated against 1TNF, 3S79 and 9V8G, producing three further complexes. The ligand identifier for this second docking panel was not specified in the available experimental record; its interactions are therefore reported separately without assigning a chemical identity.

The structures 1XP1 and 9V8G correspond to ligand-binding domains of ESR1 and PPARG, respectively (RCSB Protein Data Bank, 2004; RCSB Protein Data Bank, 2025). Binding scores were compiled in kcal/mol, and protein–ligand contacts were characterized from the recorded two-dimensional and three-dimensional interaction analyses, including hydrogen-bonding residues and distances. Accordingly, the analysis emphasizes the recorded docking scores and residue contacts rather than estimates of experimental binding constants.

3. RESULTS

3.1 Shortlisted phytochemicals

The screening yielded five prioritized compounds, four associated with *P. longifolia* and one with *N. arbor-tristis* (Table 1). The different molecular weights and drug-likeness values indicate heterogeneity in the chemical panel, supporting target-specific docking comparisons rather than a single generic activity profile.

Natural Resources for Human Health
eISSN: 2583-1194

Table 1. Molecular descriptors of the five shortlisted phytochemicals (DL, drug-likeness score; BA, predicted bioavailability score).

Plant	Compound	Molecular weight (g/mol)	DL	BA
P. longifolia	(4E,7E) -1,5,9,9-Tetramethyl-12-oxabicyclo [9.1.0] dodeca-4,7-diene	220.35	0.29	0.55
P. longifolia	6-Epi-beta-bisabolol	222.37	0.48	0.55
P. longifolia	4,8-beta-Epoxycaryophyllene	222.37	1.22	0.55
P. longifolia	Kolavenic acid	304.47	0.21	0.85
N. arbor-tristis	Nyctanthic acid	440.7	0.18	0.85

The chemical structures of the five shortlisted phytoconstituents and their predicted target-class profiles are shown in **Figures 2 and 3**. The four *P. longifolia* compounds and the *N. arbor-tristis* compound displayed different target-class distributions in the supplied prediction outputs. These plots provide a descriptive overview of predicted target classes; they do not independently establish binding, biological activity, or PCOS-specific relevance.

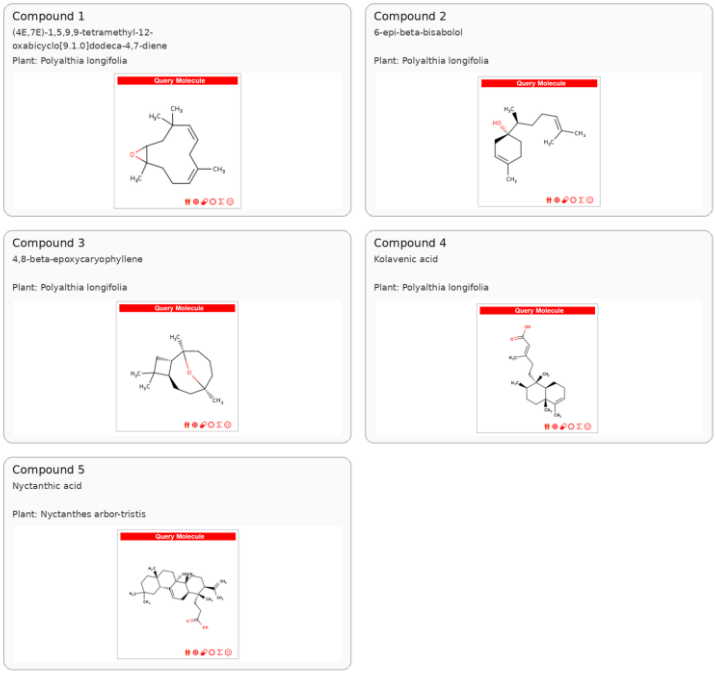


Figure 2. Chemical structures of the five shortlisted phytoconstituents: four compounds from *P. longifolia* and nyctanthic acid from *N. arbor-tristis*.

Natural Resources for Human Health
eISSN: 2583-1194

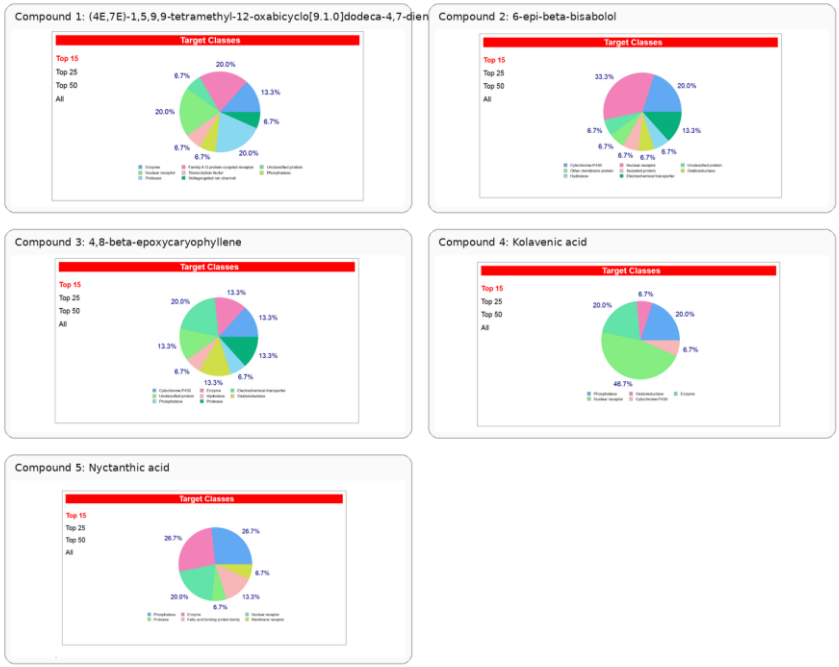


Figure 3. Predicted target-class distributions for the five shortlisted phytoconstituents, reproduced from the supplied target-class plots.

3.2 Disease-target intersections and central network nodes

Target intersection analysis identified 68 PCOS-associated genes for *P. longifolia* and 37 for *N. arbor-tristis*. This comparison concerns target-set size, not comparative therapeutic activity: the former pooled four selected constituents whereas the latter contained one. The centrality profiles repeatedly highlighted PPARG and TNF, alongside ESR1, PPARA, MAPK3, CYP19A1 and other steroid-responsive regulators. Together, these hubs motivated a dual focus on endocrine and metabolic pathways and informed the structural docking targets.

The Venn diagrams (**Figures 4 and 5**) further indicate the sizes of the input sets. For *P. longifolia*, the reported intersection comprises 68 shared targets, with 186 target-only entries and 1,054 PCOS-gene-only entries. For *N. arbor-tristis*, the intersection comprises 37 shared targets, with 63 target-only entries and 1,085 PCOS-gene-only entries. These counts describe the set intersections and should not be interpreted as measures of therapeutic potency. The corresponding STRING protein–protein interaction networks are shown in **Figures 6 and 7**.

Table 2. PCOS-associated target overlaps and prominent PPI network proteins for the two medicinal plants.

Plant	PCOS-associated overlap	Prominent network-associated proteins
P. longifolia	68	PPARG, TNF, ESR1, NR3C1, MAPK3, PPARA, CYP19A1
N. arbor-tristis	37	PPARG, TNF, CYP19A1, ESR1, CYP3A4, PPARA, MAPK3

Degree-centrality ranking of hub genes. The supplied network plots further ranked the prominent genes by degree centrality. In the *P. longifolia*–PCOS target network, PPARG and TNF ranked first and second, followed by ESR1, NR3C1, MAPK3, PPARA, CYP19A1, HIF1A, CYP3A4 and TP53. In the *N. arbor-tristis*–PCOS target network, PPARG and TNF were again the two highest-ranked nodes, followed by CYP19A1, ESR1, CYP3A4, PPARA, MAPK3, CYP17A1, AR and NR3C1. The recurrence of PPARG and TNF across both networks supports their prioritization as shared network hubs; however, degree

centrality describes network connectivity and does not establish direct compound binding or therapeutic efficacy. The degree-centrality bar charts are shown in **Figures 8 and 9**, and the hub-gene interaction networks in **Figures 10 and 11**.

Table 3. Degree-centrality ranking of the top hub genes in the two plant-associated PCOS target networks. Scores are approximate visual readings from the supplied bar charts and require confirmation against the original network export.

Plant-associated network	Rank	Hub gene	Approximate degree score
P. longifolia	1	PPARG	~41
P. longifolia	2	TNF	~38
P. longifolia	3	ESR1	~35
P. longifolia	4	NR3C1	~30
P. longifolia	5	MAPK3	~30
P. longifolia	6	PPARA	~29
P. longifolia	7	CYP19A1	~27
P. longifolia	8	HIF1A	~26
P. longifolia	9	CYP3A4	~26
P. longifolia	10	TP53	~26
N. arbor-tristis	1	PPARG	~24
N. arbor-tristis	2	TNF	~22
N. arbor-tristis	3	CYP19A1	~19
N. arbor-tristis	4	ESR1	~19
N. arbor-tristis	5	CYP3A4	~18
N. arbor-tristis	6	PPARA	~18
N. arbor-tristis	7	MAPK3	~18
N. arbor-tristis	8	CYP17A1	~17
N. arbor-tristis	9	AR	~16
N. arbor-tristis	10	NR3C1	~16

Note: Centrality scores have been estimated from the bar heights in the supplied images because the underlying numeric export was not provided. These values are provisional; replace them with exact Cytoscape/network-analysis values before submission. The gene order is transcribed from the supplied chart labels.

Natural Resources for Human Health
eISSN: 2583-1194

Input files:

List names	number of elements	number of unique elements
Targets	372	254
PCOS Genes	1168	1122
Overall number of unique elements		**1308**

Image result:

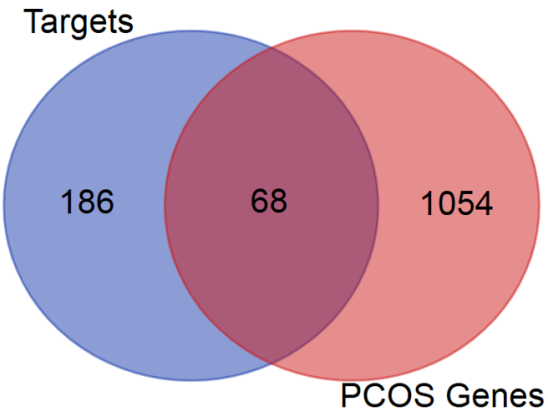


Figure 4. Venn diagram showing the overlap between *P. longifolia* compound targets and PCOS-associated genes.

Input files:

List names	number of elements	number of unique elements
Targets	100	100
PCOS Genes	1168	1122
Overall number of unique elements		**1185**

Image result:

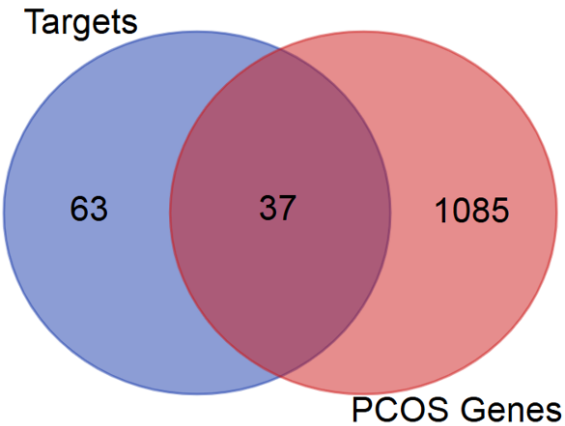


Figure 5. Venn diagram showing the overlap between *N. arbor-tristis* compound targets and PCOS-associated genes.

Natural Resources for Human Health
eISSN: 2583-1194

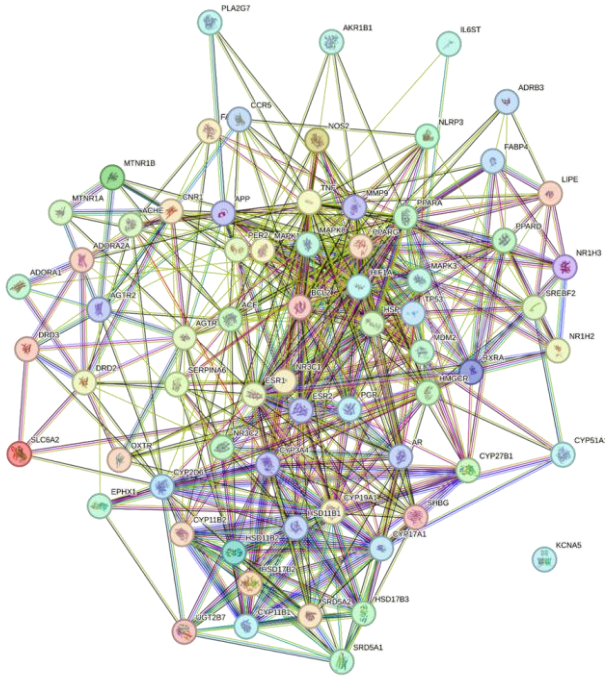


Figure 6. STRING protein–protein interaction network for the *P. longifolia* target intersection.

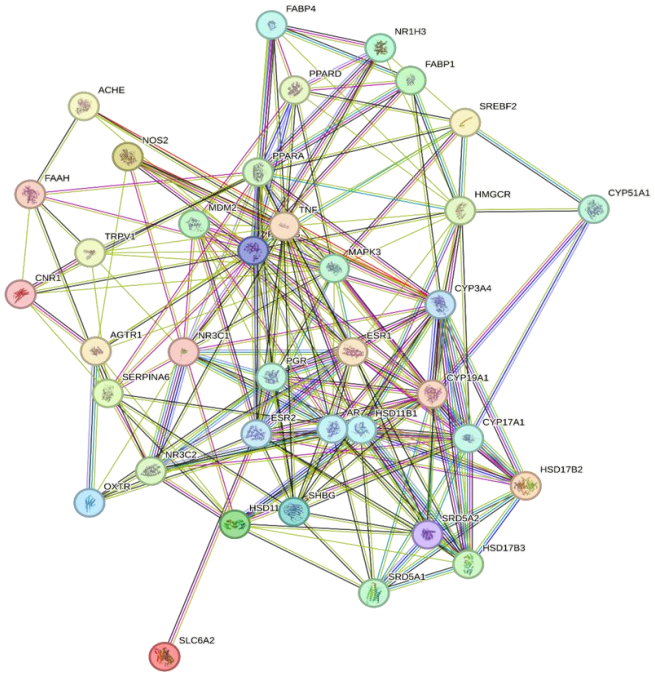


Figure 7. STRING protein–protein interaction network for the *N. arbor-tristis* target intersection.

Natural Resources for Human Health
eISSN: 2583-1194

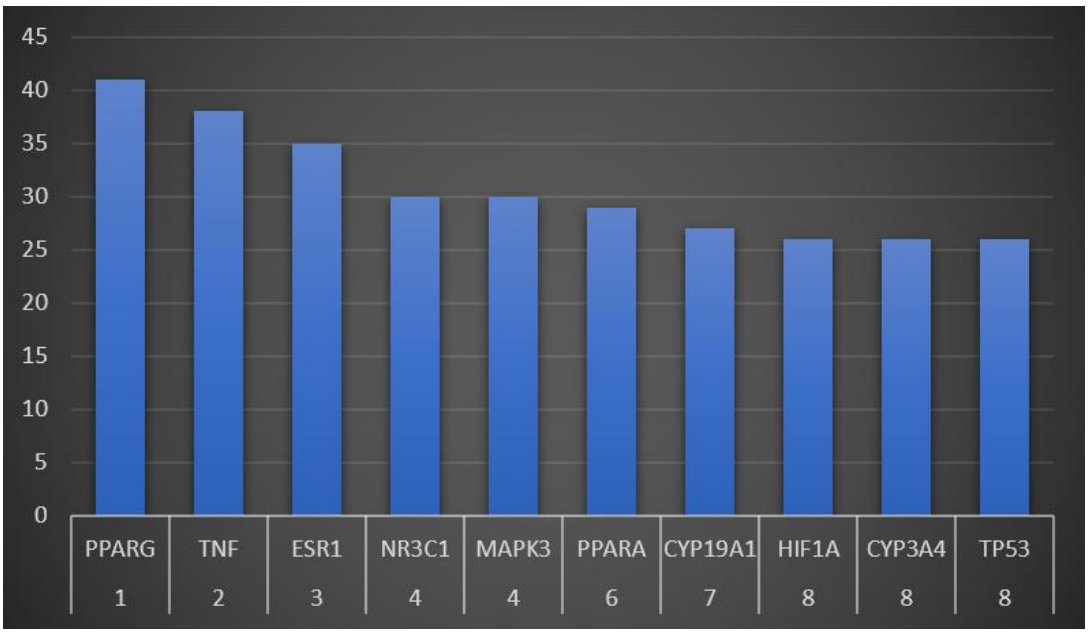


Figure 8. Degree-centrality ranking of the top hub genes in the *P. longifolia*–PCOS shared-target network.

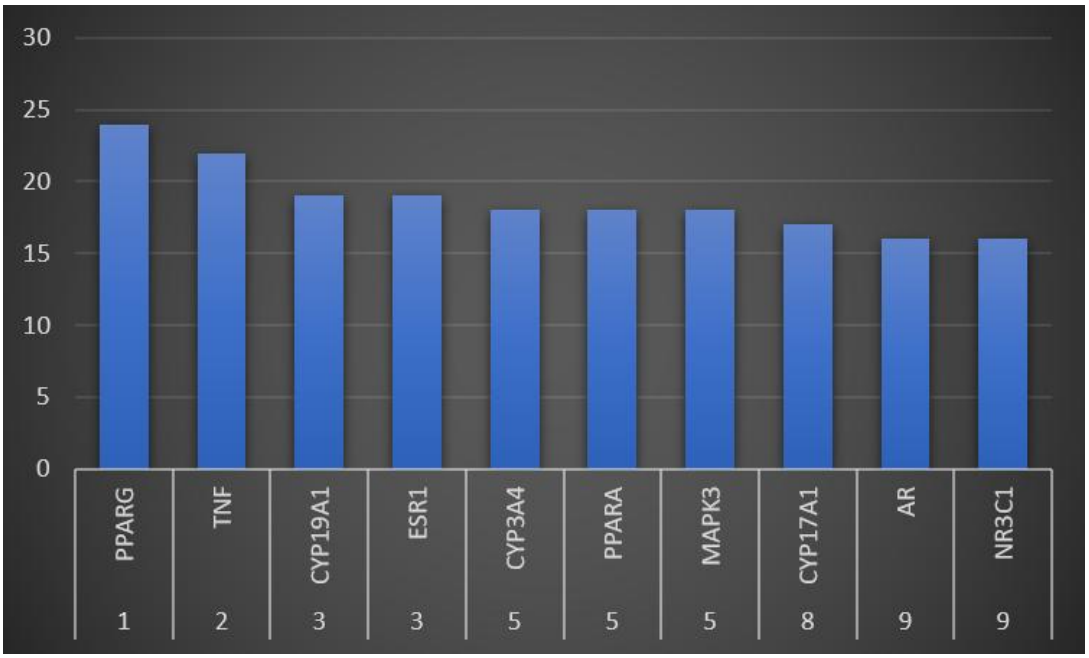


Figure 9. Degree-centrality ranking of the top hub genes in the *N. arbor-tristis*–PCOS shared-target network.

Natural Resources for Human Health
eISSN: 2583-1194

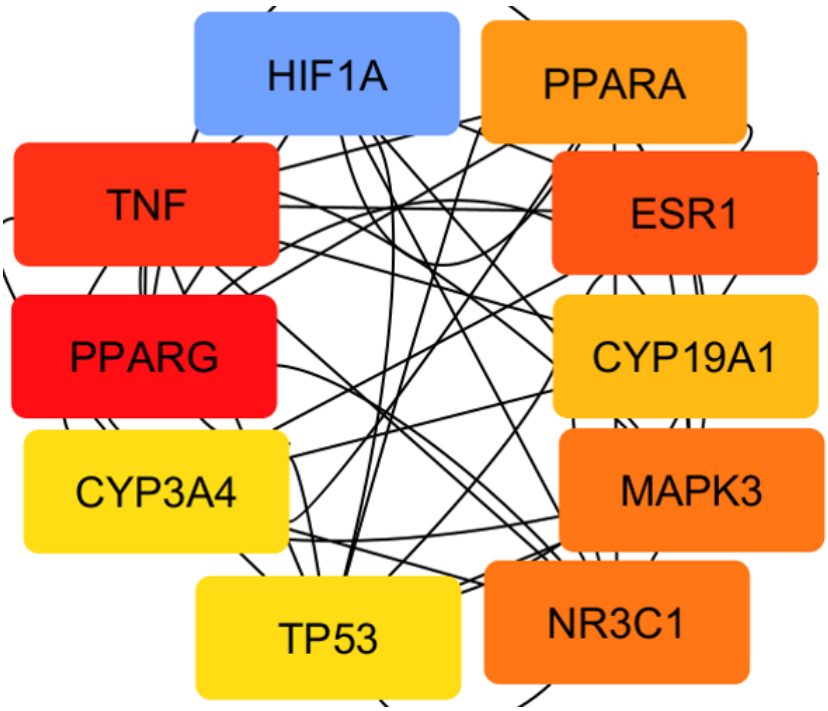


Figure 10. Hub-gene interaction network for the *P. longifolia*–PCOS shared-target set, highlighting the reported central nodes.

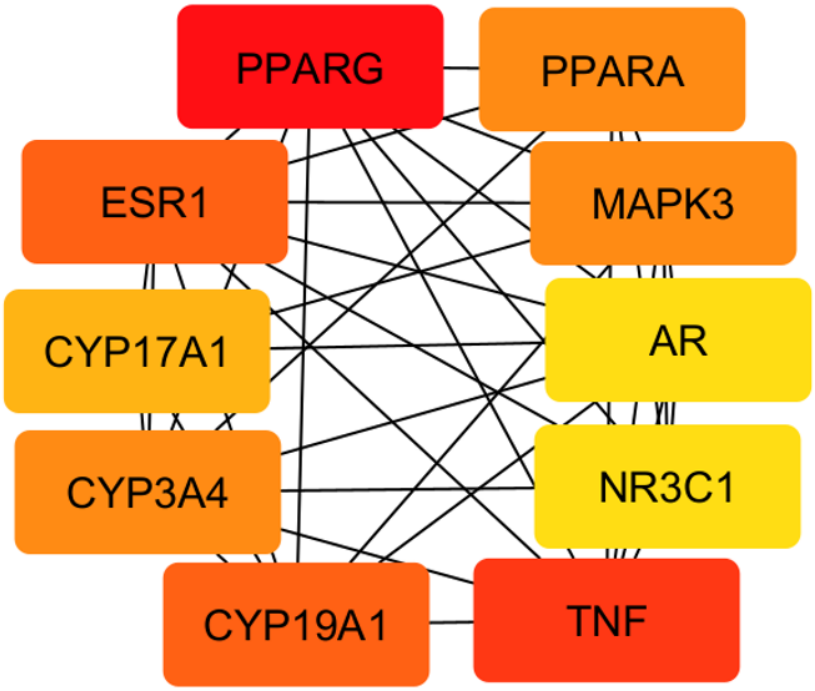


Figure 11. Hub-gene interaction network for the *N. arbor-tristis*–PCOS shared-target set, highlighting the reported central nodes.

3.3 GO and KEGG functional profiles

GO enrichment revealed consistent endocrine-related annotations across the plant-specific lists. Androgen metabolic process was significant in both *P. longifolia* (five genes; adjusted $p = 3.88 \times 10^{-5}$) and *N. arbor-tristis* (four genes; adjusted $p = 3.27 \times 10^{-4}$). Steroid binding was also strongly enriched in both sets. Steroid metabolic process reached the .05 threshold for *P. longifolia*

(adjusted p = .0136) but not for *N. arbor-tristis* (adjusted p = .0678), indicating a specific between-set difference rather than uniform support across all terms.

Table 4. Selected GO enrichment terms with gene counts and Benjamini-adjusted p-values.

Plant	GO term	Gene count	Adjusted p
P. longifolia	Androgen metabolic process	5	3.88×10^{-5}
P. longifolia	Steroid metabolic process	4	0.0136
N. arbor-tristis	Androgen metabolic process	4	3.27×10^{-4}
N. arbor-tristis	Steroid metabolic process	3	0.0678
P. longifolia	Steroid binding	11	8.07×10^{-16}
N. arbor-tristis	Steroid binding	11	1.18×10^{-18}

KEGG analysis identified steroid hormone biosynthesis among the most strongly enriched pathways for both plants, comprising 12 mapped genes for *P. longifolia* (adjusted p = 1.18×10^{-10}) and nine for *N. arbor-tristis* (adjusted p = 1.27×10^{-8}). The PPAR signaling pathway included six genes in each target set (adjusted p = 0.00378 and 0.000905, respectively). Endocrine resistance and prolactin signaling also reached statistical significance in *P. longifolia*, whereas the corresponding terms were not significant in *N. arbor-tristis* at the specified adjusted p-value threshold. These findings indicate shared steroidogenic and metabolic associations alongside plant-specific differences in enrichment (Table 5).

Table 5. KEGG pathway enrichment results for *P. longifolia* and *N. arbor-tristis*, including mapped gene counts and Benjamini-adjusted p-values.

Plant	KEGG pathway	Genes	Adjusted p
P. longifolia	Steroid hormone biosynthesis	12	1.18×10^{-10}
P. longifolia	PPAR signaling	6	0.00378
P. longifolia	Endocrine resistance	9	3.63×10^{-5}
P. longifolia	Prolactin signaling	6	0.00308
N. arbor-tristis	Steroid hormone biosynthesis	9	1.27×10^{-8}
N. arbor-tristis	PPAR signaling	6	0.000905
N. arbor-tristis	Endocrine resistance	4	0.173
N. arbor-tristis	Prolactin signaling	4	0.0952

Natural Resources for Human Health
eISSN: 2583-1194

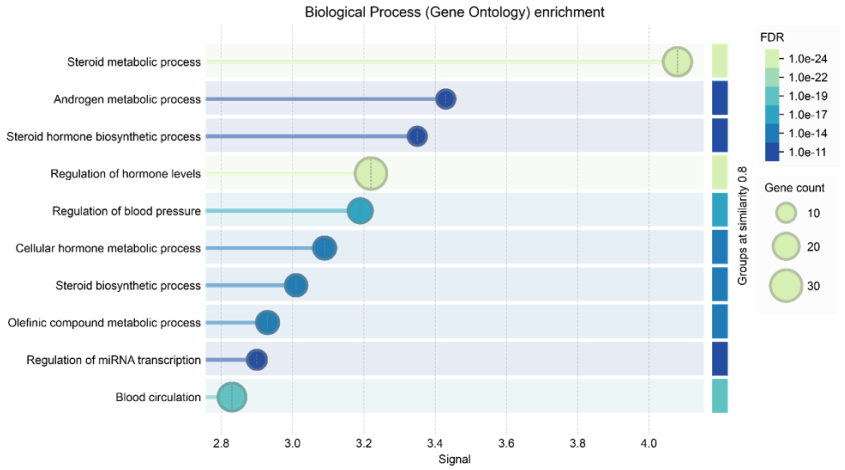


Figure 12. GO biological-process enrichment profile of *P. longifolia*-associated PCOS targets.

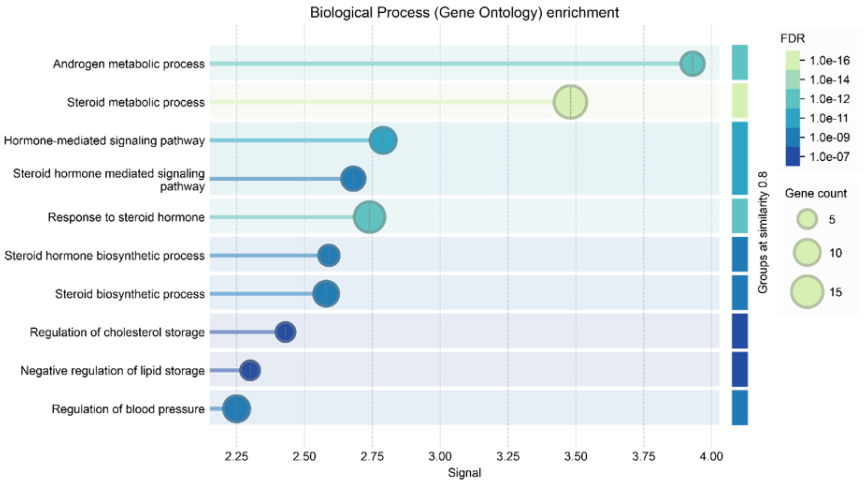


Figure 13. GO biological-process enrichment profile of *N. arbor-tristis*-associated PCOS targets.

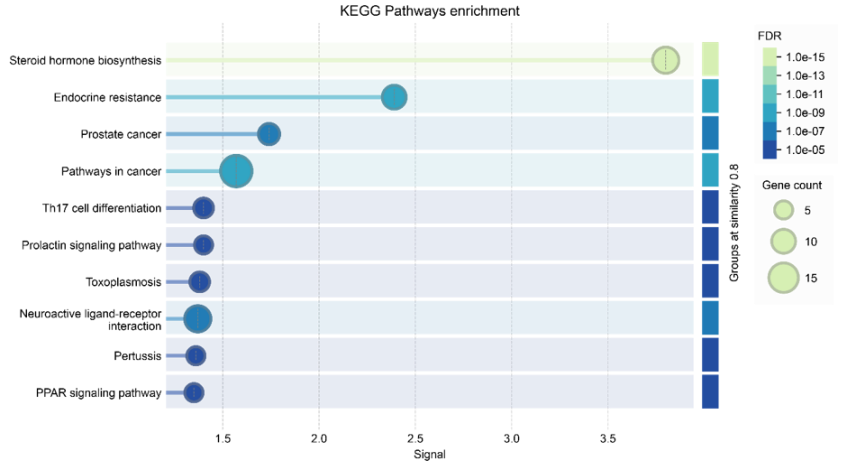


Figure 14. KEGG pathway enrichment profile of *P. longifolia*-associated PCOS targets.

Natural Resources for Human Health
eISSN: 2583-1194

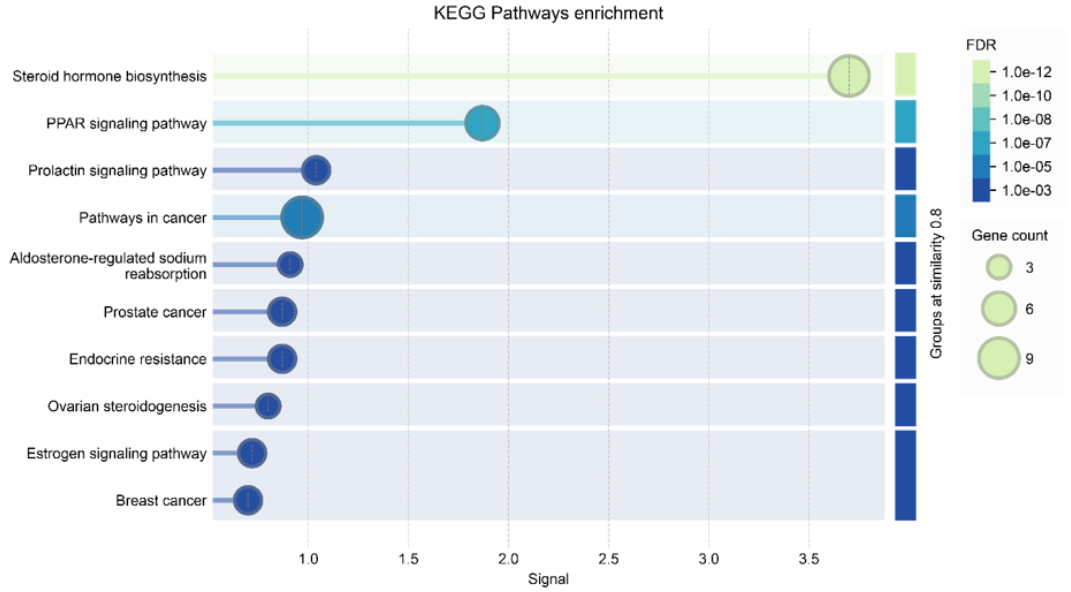


Figure 15. KEGG pathway enrichment profile of *N. arbor-tristis*-associated PCOS targets.

3.4 Molecular docking scores: 12-complex panel

Docking of the four CID-labelled phytochemicals yielded negative Vina scores across all 12 complexes (Table 6). Within the 1TNF panel, CID 6441458 had the most negative score (−8.4 kcal/mol). CID 91749887 yielded the most negative score against 1XP1 (−8.4 kcal/mol), followed by CID 6441458 (−8.2 kcal/mol). Against 9V8G, CID 6441458 showed the most negative value among these four ligands (−7.4 kcal/mol). Together, the affinity scores and interaction profiles permit comparison of ligand poses within the docking protocol, although the scores are not experimental measures of binding affinity.

Table 6. Molecular docking scores and hydrogen-bond contacts for the four CID-labelled ligands against 1TNF, 1XP1 and 9V8G.

Structure	Ligand CID	Vina score (kcal/mol)	Reported hydrogen bonds
1TNF	6441458	-8.4	None reported
1TNF	12300148	-6.4	None reported
1TNF	22559443	-6.8	None reported
1TNF	91749887	-7.2	None reported
1XP1	6441458	-8.2	ASP351 (2.94 Å)
1XP1	12300148	-7.2	None reported
1XP1	22559443	-7.5	None reported
1XP1	91749887	-8.4	None reported
9V8G	6441458	-7.4	GLN470 (3.14, 3.01 Å)
9V8G	12300148	-6.3	GLN470 (2.81 Å); LYS474 (3.20 Å)

Natural Resources for Human Health
eISSN: 2583-1194

Structure	Ligand CID	Vina score (kcal/mol)	Reported hydrogen bonds
9V8G	22559443	-6.9	VAL450 (2.87 Å); GLN454 (3.19 Å)
9V8G	91749887	-6.6	None reported

The 1XP1 complexes were dominated by nonpolar contacts involving LEU384, LEU387, MET388, LEU391, PHE404, LEU525 and neighbouring pocket residues. CID 6441458 also showed an ASP351 contact at 2.94 Å; none of the other three 1XP1 complexes had a reported hydrogen bond. In 9V8G, CID 6441458 interacted twice with GLN470 (3.14 and 3.01 Å). CID 12300148 showed contacts with GLN470 and LYS474; CID 22559443 showed reported contacts with VAL450 and GLN454. By contrast, the 1TNF table lists only LYS128 as a named interacting residue for CID 6441458 and no specific residues for the other three combinations; detailed residue-level mechanistic interpretation for those three 1TNF poses is therefore not justified by the available interaction export.

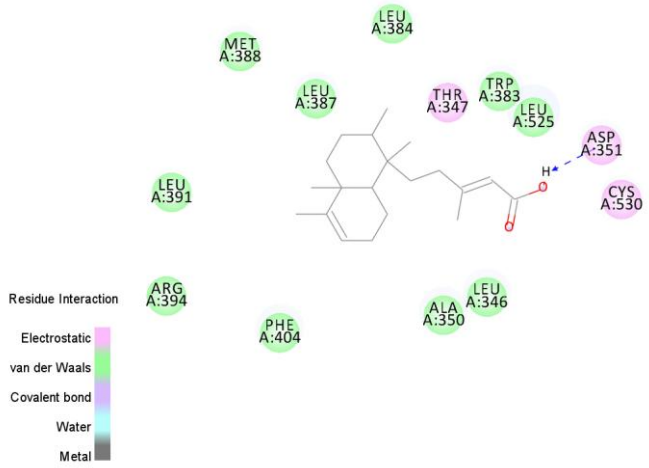


Figure 16. Two-dimensional protein–ligand interaction map for the 1XP1–CID 6441458 complex.

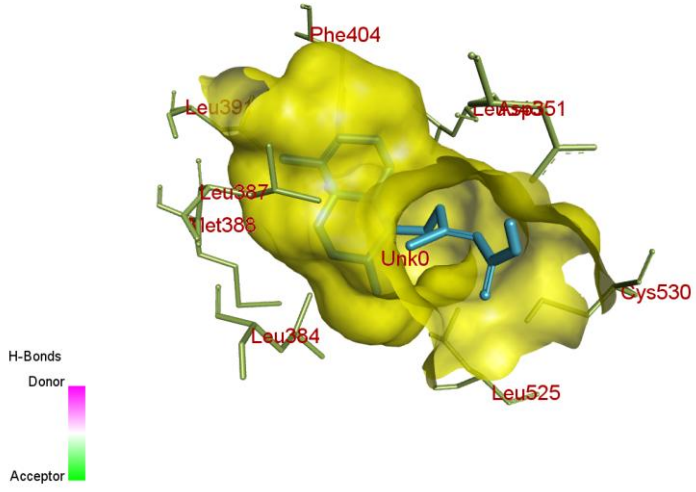


Figure 17. Three-dimensional view of the 1XP1–CID 6441458 complex.

Natural Resources for Human Health
eISSN: 2583-1194

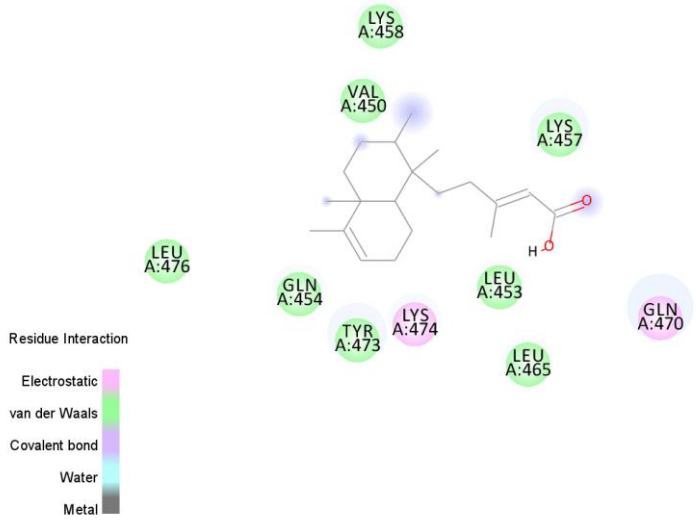


Figure 18. Two-dimensional protein–ligand interaction map for the 9V8G–CID 6441458 complex.

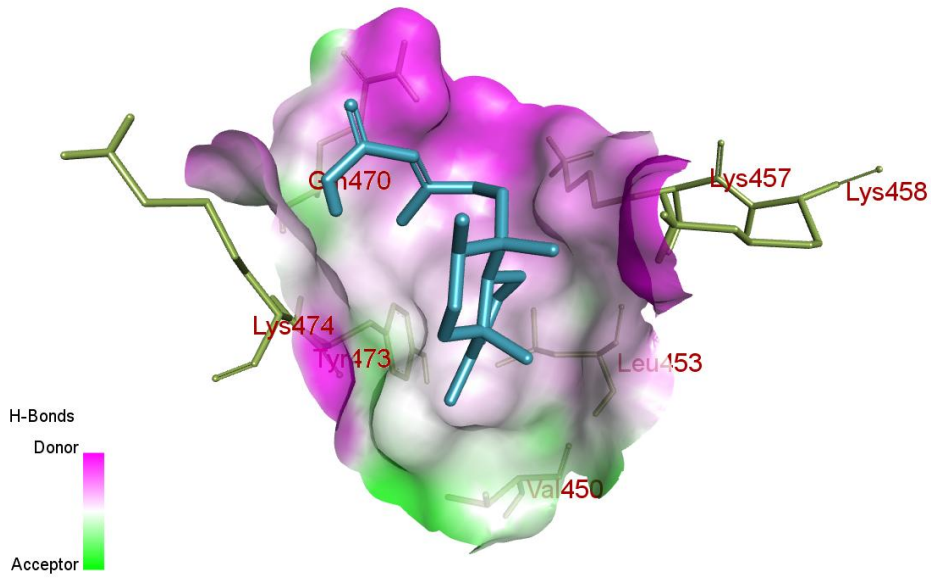


Figure 19. Three-dimensional view of the 9V8G–CID 6441458 complex.

3.5 Additional three-complex docking panel

The fifth ligand was examined against 1TNF, 3S79 and 9V8G (Table 7), producing Vina scores of −7.4, −4.7 and −7.6 kcal/mol, respectively. In the 1TNF complex, hydrogen-bond contacts involved ARG103 (3.08 and 3.19 Å), PRO106 (2.82 Å) and ALA109 (2.98 Å). The 3S79 interaction profile included HIS325 (3.27 Å), while the 9V8G complex exhibited contacts with TYR473 (2.79 Å), ASP475 (3.16 Å) and LEU476 (3.08 and 3.04 Å). These results demonstrate differences in predicted binding geometry and residue engagement among the examined structures.

Natural Resources for Human Health
eISSN: 2583-1194

Table 7. Molecular docking scores and hydrogen-bond contacts for the fifth ligand across three protein structures.

Structure	Vina score (kcal/mol)	Hydrogen-bonding residues (Å)
1TNF	−7.4	ARG103 (3.08, 3.19); PRO106 (2.82); ALA109 (2.98)
3S79	−4.7	HIS325 (3.27)
9V8G	−7.6	TYR473 (2.79); ASP475 (3.16); LEU476 (3.08, 3.04)

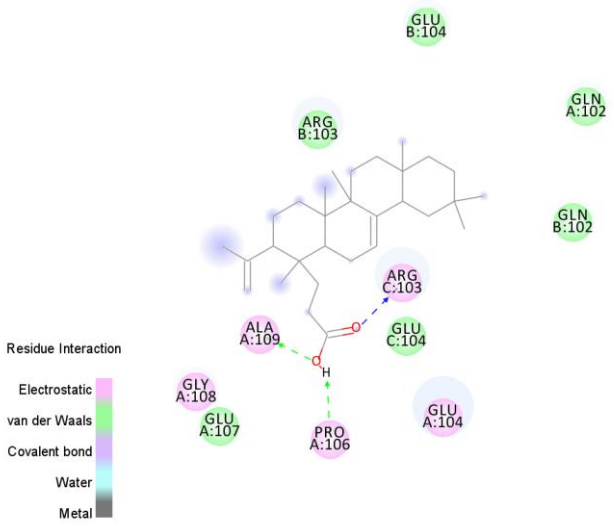


Figure 20. Two-dimensional interaction map for the fifth ligand bound to 1TNF.

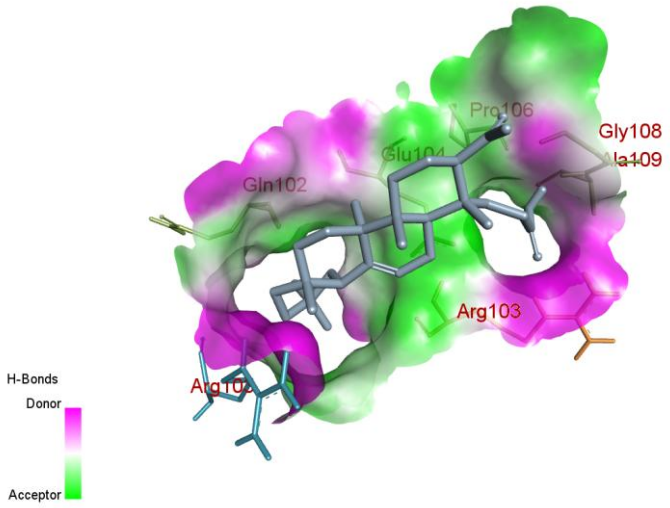


Figure 21. Three-dimensional representation of the fifth ligand–1TNF complex.

Natural Resources for Human Health
eISSN: 2583-1194

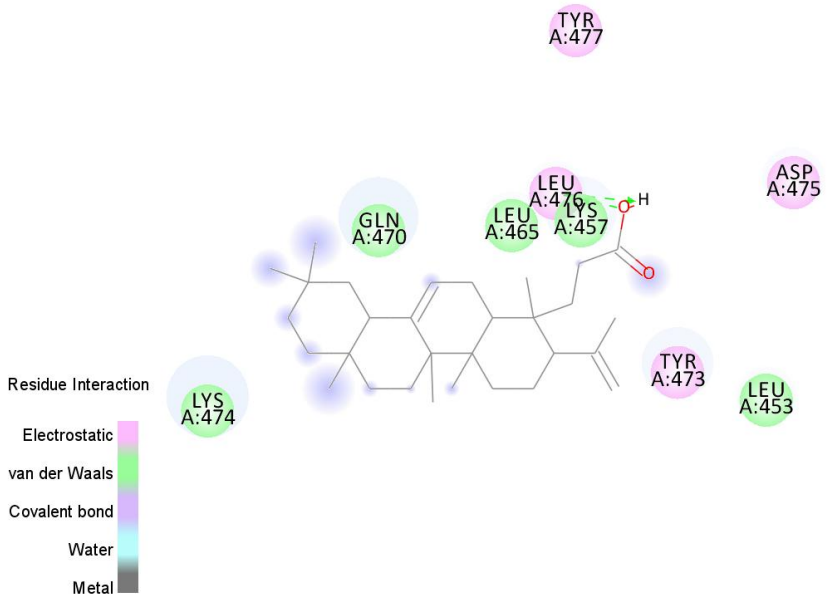


Figure 22. Two-dimensional interaction map for the fifth ligand bound to 9V8G.

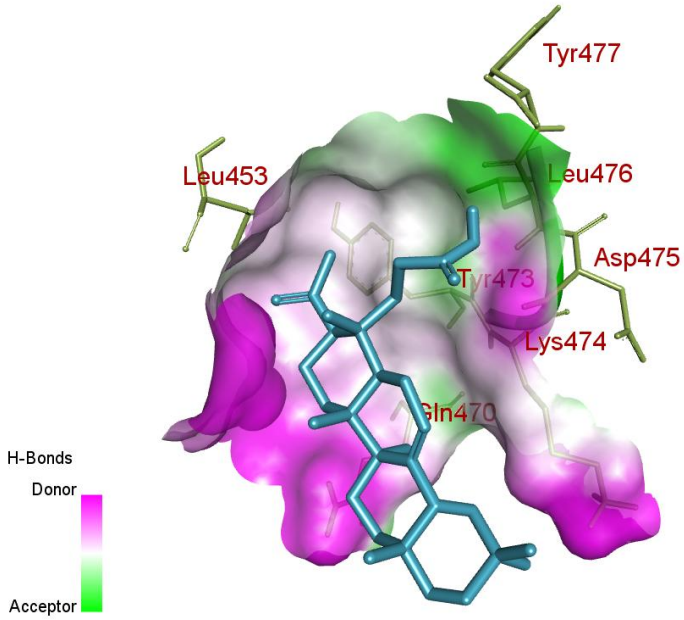


Figure 23. Three-dimensional representation of the fifth ligand–9V8G complex.

4. DISCUSSION

The integrated analysis identifies a coherent research direction centred on steroid metabolism, nuclear-receptor signaling and inflammatory networks. Highly enriched steroid hormone biosynthesis annotations suggest that selected predicted targets converge on endocrine processes relevant to PCOS. The significant PPAR enrichment in both plant datasets provides a complementary metabolic signal, consistent with the importance of insulin sensitivity and lipid homeostasis in PCOS.

Importantly, the overlap between these annotations is a property of disease-associated candidate target lists, while the docking experiments directly evaluate plausible poses within a subset of the corresponding protein structures.

ESR1 emerged as a central network candidate and a tractable structure-based target. The reported 1XP1 scores ranged from −7.2 to −8.4 kcal/mol, with hydrophobic pocket residues recurring across the four docked ligands. The ASP351 hydrogen bond for CID 6441458 provides an additional residue-level feature for follow-up. Together these observations support targeted biochemical evaluation of estrogen-receptor engagement, with the direction of functional modulation left to experimental determination. The protein identity of 1XP1 was confirmed against its RCSB entry, which describes an estrogen receptor-α ligand-binding domain (RCSB Protein Data Bank, 2004).

PPARG was common to the two plant-specific interaction networks and featured in the structurally distinct 9V8G docking panel. Across the four CID-labelled ligands, the 9V8G scores ranged from −6.3 to −7.4 kcal/mol. Polar interactions involving GLN470 and other pocket residues suggest different ligand-placement geometries, while the additional ligand scored −7.6 kcal/mol and showed contacts with TYR473, ASP475 and LEU476. Since the 9V8G RCSB structure is a PPARG ligand-binding domain, these results connect a network-level metabolic node to a specific structural model (RCSB Protein Data Bank, 2025). However, ligand binding does not resolve agonism versus antagonism, and the receptor's conformational behavior would require experimental or more extensive computational follow-up.

The TNF-related network signal calls for particular care in linking pathway hub status with docking interpretation. In the four-CID panel, the 1TNF interaction report describes very limited residue contacts despite scores as low as −8.4 kcal/mol. The additional ligand shows more explicitly reported polar contacts for 1TNF. This contrast highlights that a negative docking score, by itself, is insufficient to establish an interpretable mechanism of inhibitory TNF action. The 3S79 complex scored −4.7 kcal/mol and is best considered lower-ranked within the additional panel, without treating differences among receptor structures as a measured difference in biological efficacy.

The biological significance of the cross-plant comparison resides in concordant pathway themes, not in an assumed potency ranking. *P. longifolia* was represented by four shortlisted compounds, compared with one in *N. arbor-tristis*; therefore, its larger union of disease-associated genes is expected to be influenced by the size of the compound input. Likewise, docking comparisons require confidence in ligand stereochemistry, protonation, receptor preparation and grid definitions (Che and Zhang, 2025). Follow-up work can prioritize compound identity validation, binding assays for ESR1/PPARG-related candidates, receptor reporter assays, steroidogenic readouts and cellular assessment of toxicity or off-target effects. Such experiments would transform pathway convergence and docking poses into testable functional evidence.

5. CONCLUSION

Integrated network pharmacology and molecular docking identified candidate endocrine and metabolic targets associated with the selected phytoconstituents of *P. longifolia* and *N. arbor-tristis*. The respective disease-target intersections comprised 68 and 37 genes, with PPARG and TNF prominent in the PPI networks. Enrichment of steroid hormone biosynthesis and PPAR signaling highlighted biologically relevant pathways, while 15 docking complexes provided additional structural information about predicted ligand–protein contacts. These findings support further targeted investigation of the identified phytochemicals and their molecular interactions in PCOS-associated biological processes.

REFERENCES

[1] Abomughaid, M.M., 2026. Network pharmacology integrated molecular docking analysis identifies potential phytochemicals in Stachys lavandulifolia against polycystic ovary syndrome. *Current Pharmaceutical Design* 32(29), 2424–2438. https://doi.org/10.2174/0113816128403160250905163027

[2] Azziz, R., Carmina, E., Chen, Z., et al., 2016. Polycystic ovary syndrome. *Nature Reviews Disease Primers* 2, 16057.

[3] Banerjee, P., Kemmler, E., Dunkel, M., Preissner, R., 2024. ProTox 3.0: a webserver for the prediction of toxicity of chemicals. *Nucleic Acids Research* 52, W513–W520.

[4] Benjamini, Y., Hochberg, Y., 1995. Controlling the false discovery rate: a practical and powerful approach to multiple testing. *Journal of the Royal Statistical Society: Series B* 57, 289–300.

[5] Burley, S.K., Bhikadiya, C., Bi, C., et al., 2021. RCSB Protein Data Bank: powerful new tools for exploring 3D structures of biological macromolecules. *Nucleic Acids Research* 49, D437–D451.

[6] Che, X., Zhang, L., 2025. Blind docking methods have been inappropriately used in most network pharmacology analysis. *Frontiers in Pharmacology* 16, 1566772. https://doi.org/10.3389/fphar.2025.1566772

[7] Cheng, R., Zhu, Y., Wang, S.-K., Zong, C.-X., Zhao, H.-L., Zhang, Q., 2025. Exploration of the molecular mechanism of melatonin against polycystic ovary syndrome based on a network pharmacology approach and experimental validation. *Frontiers in Endocrinology* 16, 1528518. https://doi.org/10.3389/fendo.2025.1528518

[8] Daina, A., Michielin, O., Zoete, V., 2017. SwissADME: a free web tool to evaluate pharmacokinetics, drug-likeness and medicinal chemistry friendliness of small molecules. *Scientific Reports* 7, 42717.

[9] Daina, A., Michielin, O., Zoete, V., 2019. SwissTargetPrediction: updated data and new features for efficient prediction of protein targets of small molecules. *Nucleic Acids Research* 47, W357–W364.

[10] Day, F., Karaderi, T., Jones, M.R., et al., 2018. Large-scale genome-wide meta-analysis of polycystic ovary syndrome suggests shared genetic architecture for different diagnosis criteria. *PLOS Genetics* 14, e1007813.

[11] Dumesic, D.A., Oberfield, S.E., Stener-Victorin, E., et al., 2015. Scientific statement on the diagnostic criteria, epidemiology, pathophysiology, and molecular genetics of polycystic ovary syndrome. *Endocrine Reviews* 36, 487–525.

[12] Eberhardt, J., Santos-Martins, D., Tillack, A.F., Forli, S., 2021. AutoDock Vina 1.2.0: new docking methods, expanded force field, and Python bindings. *Journal of Chemical Information and Modeling* 61, 3891–3898.

[13] Escobar-Morreale, H.F., 2018. Polycystic ovary syndrome: definition, aetiology, diagnosis and treatment. *Nature Reviews Endocrinology* 14, 270–284.

[14] The Gene Ontology Consortium, 2019. The Gene Ontology resource: 20 years and still GOing strong. *Nucleic Acids Research* 47, D330–D338.

[15] Hopkins, A.L., 2008. Network pharmacology: the next paradigm in drug discovery. *Nature Chemical Biology* 4, 682–690.

[16] IMPPAT 2.0, 2023. An enhanced and expanded phytochemical atlas of Indian medicinal plants. *ACS Omega* https://pmc.ncbi.nlm.nih.gov/articles/PMC9996785/

[17] Lipinski, C.A., Lombardo, F., Dominy, B.W., Feeney, P.J., 1997. Experimental and computational approaches to estimate solubility and permeability in drug discovery and development settings. *Advanced Drug Delivery Reviews* 23, 3–25.

[18] O'Boyle, N.M., Banck, M., James, C.A., Morley, C., Vandermeersch, T., Hutchison, G.R., 2011. Open Babel: an open chemical toolbox. *Journal of Cheminformatics* 3, 33.

[19] RCSB Protein Data Bank, 2004. Human estrogen receptor alpha ligand-binding domain in complex with compound 15 (PDB ID: 1XP1). https://www.rcsb.org/structure/1XP1

[20] RCSB Protein Data Bank, 2025. PPARgamma ligand-binding domain in complex with PG08-NL (PDB ID: 9V8G). https://www.rcsb.org/structure/9V8G

[21] Shannon, P., Markiel, A., Ozier, O., et al., 2003. Cytoscape: a software environment for integrated models of biomolecular interaction networks. *Genome Research* 13, 2498–2504.

[22] Sherman, B.T., Hao, M., Qiu, J., et al., 2022. DAVID: a web server for functional enrichment analysis and functional annotation of gene lists (2021 update). *Nucleic Acids Research* 50, W216–W221.

[23] Stelzer, G., Rosen, N., Plaschkes, I., et al., 2016. The GeneCards Suite: from gene data mining to disease genome sequence analyses. *Current Protocols in Bioinformatics* 54, 1.30.1–1.30.33.

[24] Szklarczyk, D., Kirsch, R., Koutrouli, M., et al., 2023. The STRING database in 2023: protein–protein association networks and functional enrichment analyses. *Nucleic Acids Research* 51, D638–D646.

[25] Teede, H.J., Tay, C.T., Laven, J.J.E., et al., 2023. Recommendations from the 2023 international evidence-based guideline for the assessment and management of polycystic ovary syndrome. *Journal of Clinical Endocrinology & Metabolism* 108, 2447–2469.

[26] Trott, O., Olson, A.J., 2010. AutoDock Vina: improving the speed and accuracy of docking with a new scoring function, efficient optimization and multithreading. *Journal of Computational Chemistry* 31, 455–461. https://doi.org/10.1002/jcc.21334

[27] The UniProt Consortium, 2023. UniProt: the universal protein knowledgebase in 2023. *Nucleic Acids Research* 51, D523–D531.

[28] Warren, G.L., Andrews, C.W., Capelli, A.M., et al., 2006. A critical assessment of docking programs and scoring functions. *Journal of Medicinal Chemistry* 49, 5912–5931.